ORIGINAL ARTICLE

Generating statistically robust multipath stacking maps using congruent cells

Thomas Fuhrmann · Xiaoguang Luo · Andreas Knöpfler · Michael Mayer

Abstract Multipath effects caused by reflections in the near-field and far-field of a GNSS antenna represent a major error source in static and kinematic GNSS positioning applications. Since these effects are strongly site-specific, a generally valid and practicable analytical multipath model is still lacking. In contrast, using GNSS carrier phase observation residuals, the multipath stacking (MPS) methods are able to take site-specific conditions into account. We propose an advanced approach to performing residual-based MPS in the space domain. Being superior to most conventional attempts in which stacking cells have a fixed azimuthal resolution, our suggested method makes use of congruent cells and rigorous statistical assessments in terms of outlier detection and significance evaluation of the stacked values. The advanced stacking approach is applied to representative phase residuals from static precise point positioning. The results show that the use of congruent cells allows for MPS at high elevation angles and with a fine spatial resolution. Applying the resulting MPS maps at the residual level, both near-field and far-field effects at high and low elevation angles, respectively, can be significantly mitigated. In comparison with the conventional approach, the advanced one enables a larger reduction of about 20 % in the SD of residuals.

T. Fuhrmann (✉) · X. Luo · A. Knöpfler · M. Mayer
Geodetic Institute, Karlsruhe Institute of Technology (KIT),
Englerstr. 7, 76131 Karlsruhe, Germany
e-mail: fuhrmann@kit.edu
URL: http://www.gik.kit.edu

Present Address:
X. Luo
Leica Geosystems AG, Heinrich-Wild-Strasse,
9435 Heerbrugg, Switzerland

Introduction

GNSS are an efficient and reliable tool for accurate positioning and requires a rigorous characterization of different error effects. Despite the considerable improvements that have been achieved in modeling satellite-specific and atmospheric effects, a generally valid multipath model is still lacking. Therefore, site-specific multipath effects still represent a major error source in mm- to cm-level positioning and distort the original GNSS signal through interference. Diffuse multipath, where the reflected signal is scattered in multiple directions, exhibits noise-like behavior and is considered to be temporally uncorrelated (Braasch 1996, p. 561). In contrast, specular multipath causes systematic errors of up to a quarter of a cycle (Hofmann-Wellenhof et al. 2008, p. 157). Depending on the antenna-reflector distance, multipath effects are classified; while far-field effects show short-periodic properties (up to half an hour; Seeber 2003, p. 317) and can be averaged out over a long observation period, the near-field effects possess nonzero mean and long-periodic characteristics of up to several hours (Dilßner et al. 2008) and can be determined by absolute antenna calibration (Wübbena et al. 2011).

A straightforward option for multipath mitigation is to prevent and reduce reflections in the vicinity of the receiver antenna, e.g., site selection, microwave-absorbing materials (Ning et al. 2011). Other mitigation options can be classified into (1) antenna design (Bedford et al. 2009), e.g., polarization-related antenna gain pattern, choke rings, ground planes, antenna arrays, (2) receiver architecture, e.g., correlator techniques (Ray 2006; Lau 2012), and (3)

Table 1 Multipath mitigation approaches based on data processing

Approach	Further readings
In situ calibration	Wanninger and May (2000), Park et al. (2004), Wübbena et al. (2011)
Wavelet-based multipath reduction	Zhong et al. (2008)
SNR-based multipath mitigation	Bilich and Larson (2007), Rost and Wanninger (2009)
LMS adaptive filter	Liu et al. (2011)
Improved stochastic modeling	Lau and Cross (2006), Luo et al. (2008), Luo (2013, Chap. 8)
Computational electromagnetic modeling	Fan and Ding (2006)
Sidereal stacking and filtering	Agnew and Larson (2007), Ragheb et al. (2007), Lidberg et al. (2009), Lau (2012), Luo (2013, Chap. 7)

data processing. The third category is preferred for handling multipath errors in carrier phase measurements and includes the approaches summarized in Table 1.

Since multipath effects are strongly site-specific, the analytical modeling is difficult. In contrast, empirical methods such as stacking enable a flexible multipath characterization that copes with site-specific properties. Making use of observation residuals, a sophisticated, cell-related stacking approach should be (1) applicable to all satellite-based navigation systems, (2) capable of detecting both far-field and near-field multipath signals, (3) robust against satellite maneuvers, (4) independent of GNSS equipment and data sampling rates, (5) usable in real-time and post-processing, and (6) suitable for easy assessment of site quality.

Taking these aspects into account, we propose a method for generating statistically robust site-specific multipath stacking (MPS) maps using congruent cells. It focuses on high-precision static GNSS positioning and is applicable to continuously operating GNSS networks. In "Advanced stacking approach", the proposed stacking approach is presented considering both geometrical and statistical aspects. "Study area and GNSS data analysis" describes the area of a case study and the GNSS data analysis carried out in precise point positioning (PPP) mode. In "Results and discussion", based on representative PPP residuals, the advantages of the suggested multipath characterization are demonstrated in comparison with conventional approaches employing a fixed azimuthal resolution. Finally, "Conclusions and outlook" provides concluding remarks and an outlook on future research.

Advanced stacking approach

The main objective of this study was to develop a sophisticated approach for generating MPS maps to

efficiently assess and mitigate the limiting site-specific effects in static GNSS positioning. Apart from achieving multipath reduction, the resulting MPS maps can also be used to correct the remaining errors in receiver antenna models. Since the various GNSS have different orbit repeat times, e.g., GPS: approx. 1 sidereal day, GLONASS: approx. 8 sidereal days, Galileo: approx. 10 sidereal days (Eissfeller et al. 2007), the spatial stacking variant is chosen to ensure applicability to all GNSS. If multipath errors are not considered during the course of GNSS data analysis, they remain in residuals and bias parameter estimates, e.g., site coordinates. The advanced stacking process makes use of carrier phase residuals from PPP (Zumberge et al. 1997) and enables—in contrast to differential GNSS—an individual site-satellite multipath detection, which is easily interpretable with respect to signal direction. Being superior to conventional methods using stacking cells with a fixed azimuthal resolution, the proposed MPS method applies congruent cells, along with rigorous statistical assessments. Assuming that all remaining effects, e.g., atmosphere, vary randomly over time the proposed stacking technique is described considering both geometrical and statistical aspects.

Geometrical aspects

Most common approaches to spatially mapping and stacking of site-specific multipath effects employ a constant resolution in azimuth and elevation direction, e.g., $5° \times 2°$ (Wanninger and May 2000; Lidberg et al. 2009) or $1° \times 1°$ (Iwabuchi et al. 2004; Bilich and Larson 2007; Bender et al. 2008). The main disadvantage of specifying a fixed azimuthal resolution is that the arc of the horizontal circle decreases with increasing elevation angle, schematically illustrated in Fig. 1, i.e., $b_0 > b_1 > b_2$ for $dA_0 = dA_1 = dA_2$. This leads to a decreasing size of the stacking
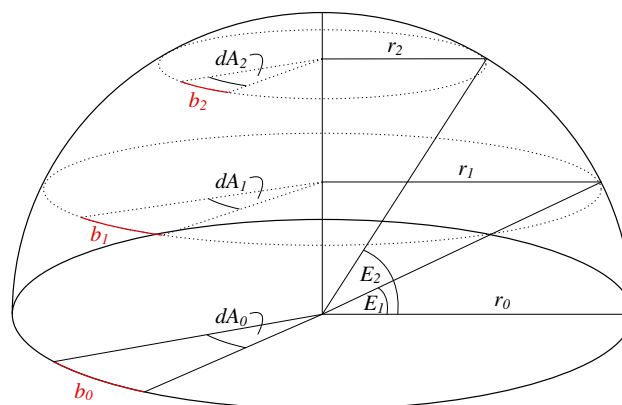

Fig. 1 Variation of azimuthal increments b_i with constant azimuth angles depending on elevation angles E_i

cell as the elevation angle increases. Accordingly, fewer residuals are included in a stacking element at higher elevation angles. Considering that GNSS signals from high-elevation satellites may be distorted significantly by near-field multipath effects, appropriate cell sizes are required to obtain reliable stacking results over the entire antenna hemisphere.

In this study, MPS maps are generated using almost congruent cells, which have a similar shape and size. Since the increment in elevation direction is kept constant, the congruence of stacking cells is realized by means of a variable azimuthal resolution. As Fig. 1 shows, the arc of the horizontal circle b_i can be expressed depending on the elevation angle E_i as

$$b_i = dA_i \cdot r_i = dA \cdot r_0 \cdot \cos E_i \qquad (1)$$

where dA_i is the azimuthal increment in degrees and r_0 is the radius of the maximum horizontal circle. For a constant azimuthal resolution, i.e., $dA_i = dA_0$, b_i decreases with increasing E_i, since the cosine function is monotonically decreasing in the interval $[0°, 90°]$. In order to satisfy the congruence condition, namely $b_i = b_0$, the variable azimuthal increment dA_i and the associated integer number of cells C_i can be derived as

$$dA_i = \frac{dA_0}{\cos E_i} \text{ and } C_i = \text{ROUND}\left(\frac{360°}{dA_i}\right) \qquad (2)$$

respectively, where ROUND(x) denotes the rounding of x to the nearest integer. For representative elevation angles of the cell center E_i, Table 2 compares the azimuthal cell numbers C_i and arc lengths b_i determined using the conventional and proposed approaches, where $dA_0 = 1°$, $r_0 = 180/\pi$, and the increment in elevation direction is 1°. In contrast to the proposed MPS approach, using a fixed azimuthal resolution of 1°, each horizontal circle has the same number of stacking elements, i.e., $C_i = 360$. However, as E_i increases from 0.5° to 80.5°, the arc length of the azimuthal increment b_i significantly decreases from 1 to 0.17 rad. This decrease is particularly observable for $E_i > 50°$. Such an effect is usually neglected in the conventional multipath analysis by assuming that site-specific errors are dominant at low elevation angles of up to 50°

(Wanninger and May 2000). Making use of a variable azimuthal resolution, the proposed solution produces different cell numbers C_i ranging between 59 and 360 for E_i between 80.5° and 0.5°. Despite increasing elevation angles, the resulting arc lengths b_i exhibit similar values, producing almost congruent cells for accurately characterizing site-specific effects at both low and high elevation angles.

Statistical aspects

The site-specific MPS map is generated by computing the arithmetic mean of the PPP residuals being located in a certain azimuth-elevation interval. Since the cell mean value depends on the sample data, e.g., sample size, and is sensitive to outliers, statistical assessments are performed during the stacking procedure to derive representative and reliable cell means. This marks a significant improvement in the proposed approach in comparison with previous attempts. Under the assumption that the residuals $\{x_1, x_2, \ldots, x_n\}$ are independent and normally distributed as $N(\mu, \sigma^2)$ then the expected value of the mean $\bar{X}$ is $E(\bar{X}) = \mu$, the SD is

$$\sigma_{\bar{X}} = \sigma/\sqrt{n} \qquad (3)$$

Applying the standardization to the mean $\bar{X}$, it follows according to Snedecor and Cochran (1980, p. 45) that

$$Y \sim = \frac{\bar{X} - \mu}{\sigma/\sqrt{n}} \sim N(0, 1) \qquad (4)$$

As a result, the $(1 - \alpha)$ confidence interval for μ can be written as

$$\left[\bar{X} - \underbrace{z_{1-\alpha/2} \cdot \sigma/\sqrt{n}}_{e}, \quad \bar{X} + \underbrace{z_{1-\alpha/2} \cdot \sigma/\sqrt{n}}_{e} \right] \qquad (5)$$

where z_q denotes the q-quantile of the standard normal distribution, e is referred to as the absolute error, and α is the significance level corresponding to probability of committing a Type I error. For a given e in (5), one can compute the minimum number of residuals in one stacking cell as

Table 2 Comparison of the azimuthal cell numbers C_i and arc lengths b_i based on fixed and congruent cell solutions

Approach	$E_i[°]$	0.5	10.5	20.5	30.5	40.5	50.5	60.5	70.5	80.5
Fixed	C_i [-]	360	360	360	360	360	360	360	360	360
Congruent	C_i [-]	360	354	337	310	274	229	177	120	59
Fixed	b_i [rad]	1.00	0.98	0.94	0.86	0.76	0.64	0.49	0.33	0.17
Congruent	b_i [rad]	1.00	1.00	1.00	1.00	1.00	1.00	1.00	1.00	1.01

The azimuthal resolution is set to 1° × 1° for the fixed solution and to $dA_i × 1°$ for the congruent solution according to (2) with $dA_0 = 1°$, $r_0 = 180/\pi$. The increment in elevation direction is given with respect to the cell center

$$n_{\min} = \text{ROUND}\left(\frac{z_{1-\alpha/2}^2 \cdot \sigma^2}{e^2}\right) \qquad (6)$$

Taking $\alpha = 5\%$ and $\sigma = 2\,e$ as an example, $n_{\min}$ is equal to 15. It should be noted that for multipath mitigation using cell-based stacking methods, the choice of an appropriate $n_{\min}$ depends on various factors such as the total number of residuals to be stacked, the cell resolution in azimuth and elevation direction, as well as the specified significance level and error tolerance. In this context, it can be seen that the geometrical and statistical aspects are correlated with each other.

Prior to conducting the stacking process, residual outliers are handled in a statistically rigorous manner by means of a three-step iterative procedure consisting of identification, verification, and elimination. Assuming that GNSS observations are normally distributed, outlying residuals in a single cell are first identified using the well-known 3-sigma rule. More precisely, the residual x_I^i from cell I is considered as an outlier if

$$|x_I^i - \bar{x}_I| > 3 \cdot s_I \qquad (7)$$

where $\bar{x}_I$ and s_I are the corresponding sample mean and SD, respectively. Since the sample variance is more sensitive to outliers than the sample mean, the F-test is used in the verification step to evaluate the influence of the detected outliers on the sample variance (Snedecor and Cochran 1980, p. 98). Thereby, the residual data sets with and without outliers are denoted as $x_{I,1}$ and $x_{I,2}$, respectively. Since the sample variance $s_{I,1}^2$ is generally larger than $s_{I,2}^2$, the one-sided F-test for equality of variances is carried out based on the test statistic

$$T_F = \frac{s_{I,1}^2}{s_{I,2}^2} \sim F(f_{I,1}, f_{I,2}) \qquad (8)$$

with $f_{I,1} = n_{I,1} - 1$ and $f_{I,2} = n_{I,2} - 1$ degrees of freedom, where $n_{I,1}$ and $n_{I,2}$ are the sample sizes of $x_{I,1}$ and $x_{I,2}$, respectively. If $s_{I,1}^2$ is significantly larger than $s_{I,2}^2$, i.e., rejecting the null hypothesis of equal variances, the residual x_I^i with the greatest distance to the mean $\bar{x}_I$ is removed in the elimination step. Given that there are still enough residuals in cell I (i.e., $n_I \geq n_{\min}$), this three-step procedure is iterated until all significant outliers are eliminated. The final stacked values are actually the arithmetic means of the outlier-free residuals.

The last component of the statistical assessments is to check whether the cell mean residual $\bar{x}_I$ differs significantly from zero. This is accomplished by calculating the corresponding $(1 - \alpha)$ confidence interval as

$$\left[-t_{n_I-1,\,1-\alpha/2} \cdot s_I/\sqrt{n_I},\ t_{n_I-1,\,1-\alpha/2} \cdot s_I/\sqrt{n_I}\right] \qquad (9)$$

where $t_{f,q}$ denotes the q-quantile of Student's t-distribution with f degrees of freedom. The stacked value $\bar{x}_I$ is significantly different from zero if $\bar{x}_I$ lies outside this interval.

Stacking process

The input data of the stacking process, see Fig. 2, are residuals of the ionosphere-free (L3) phase observations, obtained from a static GPS data analysis in PPP mode. Based on the user-specified resolution in azimuth and elevation direction, the congruent stacking cells are constructed for allocating the residuals according to their azimuth and elevation angles. If the minimum number of residuals given by (6) is fulfilled, the cell sample mean and SD are computed, which are then used for the three-step iterative outlier detection, see (7) and (8). After all significant outliers are removed, the stacked values are determined for each cell by calculating the arithmetic means of the outlier-free residuals. Next, the statistical significance of each stacked value is verified by means of (9), and only those that are significantly different from zero are used to generate site-specific MPS maps. In comparison with conventional spatial stacking approaches that assume a fixed azimuthal resolution, the proposed variant enables an advanced cell construction and a rigorous statistical evaluation.

Study area and GNSS data analysis

To verify the performance of the suggested stacking method, a case study is carried out in the area of the GNSS
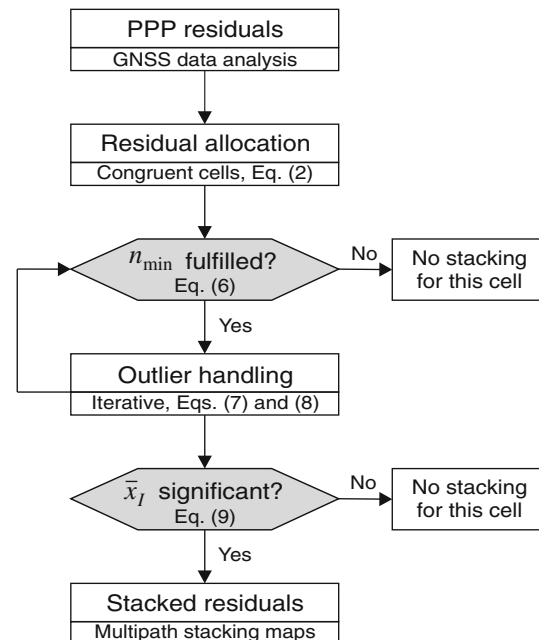
Fig. 2 Flowchart of the proposed stacking approach using congruent cells

Upper Rhine Graben Network (GURN; Mayer et al. 2012), located in Central Europe. The current GURN consists of about 80 permanently operating reference sites for high-precision determination of recent crustal movements (Fuhrmann et al. 2012) and atmospheric water vapor fields (Fuhrmann et al. 2010; Alshawaf et al. 2012). The data quality of all GURN sites was previously evaluated (Knöpfler et al. 2010), thereby detecting significant multi-path effects at both low and high elevation angles, which has to be handled carefully so that they neither propagate into coordinate estimates nor create velocity biases (King and Watson 2010).

Using the Bernese GPS Software Version 5.0 (Dach et al. 2007), 30 days (DOY2008:276-305; October 2–31, 2008) of 30-s GPS measurements are analyzed in PPP mode. Table 3 lists the most important specifications of the GPS data analysis. In terms of external data and correction models, the precise and up-to-date products from International GNSS Service (IGS) and Center for Orbit Determination in Europe (CODE) are incorporated. The resulting residuals are then used to generate site-specific MPS maps.

Results and discussion

This section first compares the fixed azimuth and congruent cell solutions under geometrical aspects. Next, representative examples of MPS maps produced by the advanced

Table 3 Specifications of the PPP data analysis

Geodetic datum	IGS05, epoch 2000.0
Processing time interval	DOY2008:276-305, daily solution
GPS observation data	30-second phase zero-differences (L3)
Observation weighting model	Elevation-dependent ($\sin^2 E$; Dach et al. 2007, p. 144)
Elevation cut-off angle	$10°$
EOP/satellite orbit/clock	Final CODE products (24 h/15 min/ 30 s)
Troposphere a priori model	Saastamoinen model (Saastamoinen 1973)
Tropospheric mapping function	Niell mapping functions (dry, wet; Niell 1996)
Time span for troposphere parameters	1 h for final solutions
Time span for tropospheric gradients	24 h (Dach et al. 2007, p. 249)
Satellite antenna correction	IGS absolute antenna model (Schmid et al. 2007)
Receiver antenna correction	Absolute calibration (individual or IGS type-specific)

EOP Earth orientation parameters

stacking approach are presented. Finally, the MPS maps are applied to residuals to illustrate the differences to stacking with a fixed azimuthal resolution.

Geometrical aspects

In order to obtain statistically reliable stacked values, the minimum number of residuals per cell n_{min} given by (6) is set to 15. Taking the almost obstacle-free GURN site TÜBINGEN as an representative example, the stacking of 10 consecutive days (DOY2008:276-285) of 239,550 PPP residuals yields 1,051 cells (7.3 %) with a number of residuals less than n_{min} if a fixed elevation and azimuth resolution of $1° \times 2°$ is used (14,400 cells in total). In this case, a total of 7,658 residuals (3.2 %) are excluded from the stacking process. In contrast, employing the proposed approach using congruent cells, where $dA_0 = 2°$ and the azimuth increment dA_i increases with increasing elevation angle, see Fig. 1 and 2, only 324 cells (3.8 %) of 8,525 cells in total do not fulfill the criterion of $n_{min} = 15$. Accordingly, a total of 2,198 residuals (0.9 %) do not contribute to generating site-specific MPS maps. This actually represents a significant reduction of unused residuals by about 70 %.
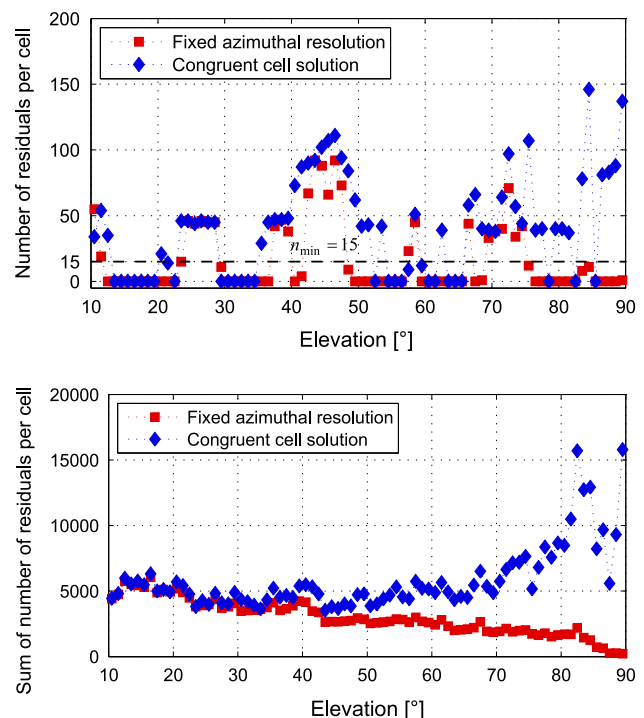

Fig. 3 Number of residuals per cell and its sum for an elevation and azimuth resolution of $1° \times 2°$ (site TÜBINGEN, DOY2008:276-285): *top panel* single azimuthal section with $A_i = 146°$, *bottom panel* all azimuthal sections with $A_i = 0°, 2°, 4°,..., 358°$

Considering the same example, Fig. 3 compares the number of residuals per cell and its sum with respect to the applied stacking approach. For a representative fixed azimuth of $A_i = 146°$ and variable elevation angles E_i, Fig. 3, top, clearly illustrates the benefit of using congruent cells at $E_i > 35°$. Taking all azimuthal sections with $A_i = 0°, 2°, 4°, \ldots, 358°$ into account, Fig. 3, bottom, shows that a fixed azimuthal resolution leads to a strong decrease in the total number of residuals, particularly at higher elevation angles. Applying the congruent cell approach, the sum of number of residuals per cell varies at a relatively constant level for $E_i < 75°$, and significantly larger amounts of high-elevation residuals are available for stacking. In addition, a statistical testing of residuals as proposed in "Statistical aspects" is more valid using the congruent cell approach, which represents the spatial and statistical distribution of residuals superiorly.

Multipath stacking maps

The reliability of the stacked values or MPS maps strongly depends on the number of residuals per cell, which is related to the user-specified resolution in azimuth and elevation direction. Generally speaking, for the same database, a higher (lower) resolution results in a smaller (larger) number of residuals allocated to cells. To demonstrate the influence of cell resolution on multipath characterization, Fig. 4 shows the 3D MPS maps generated using different resolutions for the GURN site FRETTE. As can be seen from Fig. 4a, a fine resolution of $1° \times 1°$ (elevation $\times$ dA_0; see Fig. 1) allows for the detection of

Fig. 4 3D visualization of site-specific MPS maps using congruent cells. Site FRETTE, DOY2008:276-283, *white cells* no stacked values, *grey cells* "north hole" area in which no satellites are visible. Resolutions: **a** $1° \times 1°$ (elevation $\times$ azimuthal resolution dA_0; see Fig. 1), **b** $1° \times 2°$, **c** $2° \times 2°$, **d** $2° \times 4°$, **e** $4° \times 4°$
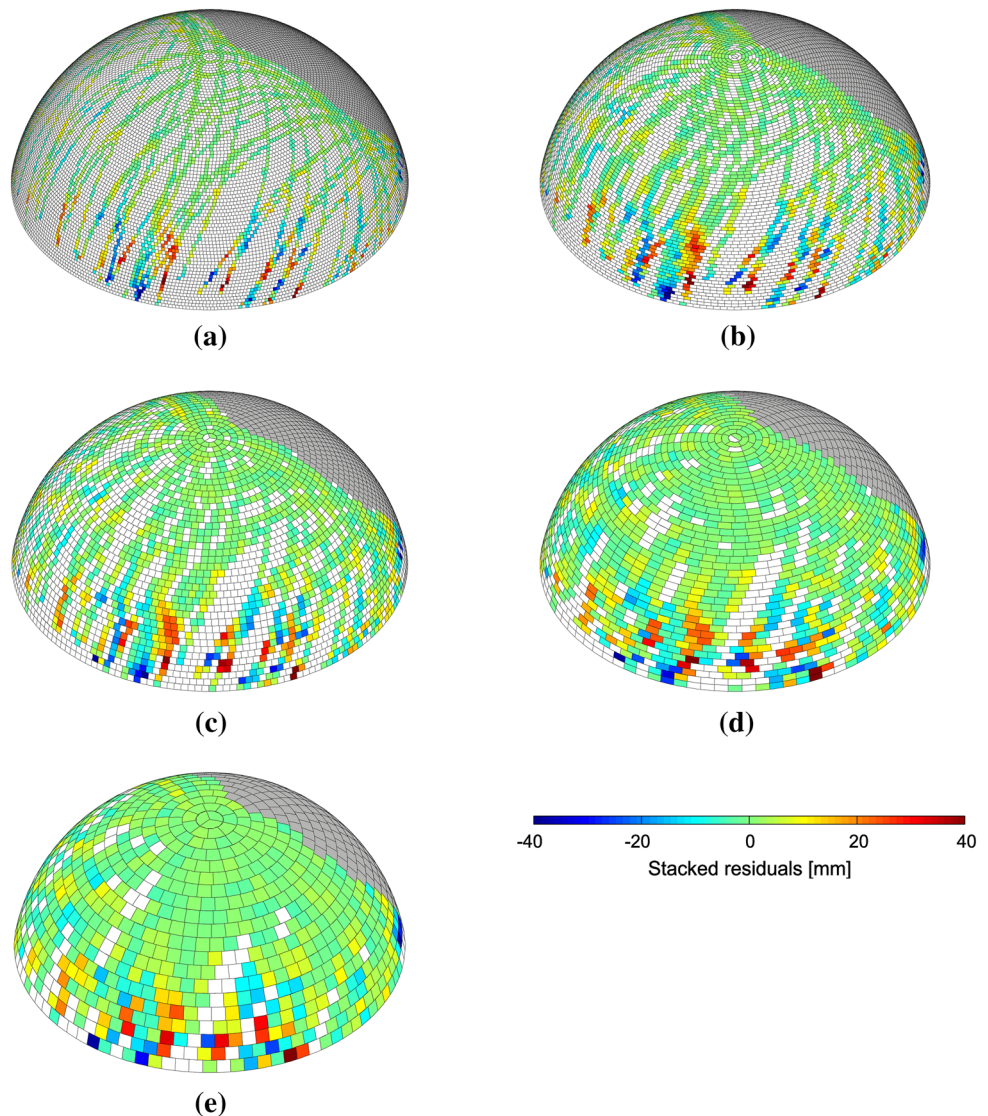
the most significant multipath effects, but leaves a large amount of cells unstacked. In contrast, coarse resolutions, such as $2° \times 4°$ and $4° \times 4°$ depicted in Fig. 4d and e, respectively, provide inaccurate multipath characterization due to the fact that a stacked value is not representative for the whole cell. By comparing Fig. 4b and c with each other, the resolution $1° \times 2°$ seems to be a good compromise between geometrical representation of multipath effects and statistical reliability. This resolution is used below for the validation of the generated MPS maps.

Validation of multipath stacking maps

After subtracting the stacked values (see Fig. 4) from the corresponding residuals, the congruent cell approach for generating MPS maps is first verified in the space and time domains. Taking the GURN site SELESTAT for example, Fig. 5 compares the residuals on DOY2008:278 before and after correcting multipath effects, where a total of approx. 25,000 PPP residuals from 10 consecutive days (DOY2008:276-285) contribute to the associated MPS map. In Fig. 5a, an oscillating pattern is visible at low elevation angles ($E < 50°$), indicating strong multipath effects (Rost and Wanninger 2009). However, after applying multipath corrections in form of a MPS map, the oscillations are significantly reduced (see Fig. 5, bottom). In addition, the large residual values displayed in red and blue colors in Fig. 5, top, almost disappear in Fig. 5, bottom.

The impact of multipath reduction on residuals is also studied in the time domain. For the site SELESTAT and GPS satellite PRN 6, Fig. 6 compares the residual time series on DOY2008:285 before and after employing the MPS map. One can easily discern that significant multipath reduction is achieved at low elevation angles ($E < 50°$), particularly in the descending part of the satellite arc from 19 to 20 h. Furthermore, noticeable corrections are also obtained at higher elevations, which can be explained by the more sophisticated congruent cell construction proposed in this study. These promising results of multipath mitigation at the residual level motivate the application of MPS maps at the observation level in future research.

In addition, the influence of applying MPS maps is statistically analyzed by computing per satellite the arithmetic means and SDs of residuals for each site. As an example, Fig. 7 illustrates the statistical characteristics obtained for the site SELESTAT, where 10 days of PPP residuals are considered. In Fig. 7, top, the mean values of the corrected residuals exhibit smaller variations and are closer to zero than those of the uncorrected residuals. This implies a great potential of MPS maps for reducing biases in GNSS parameter estimates. As can be seen from Fig. 7,
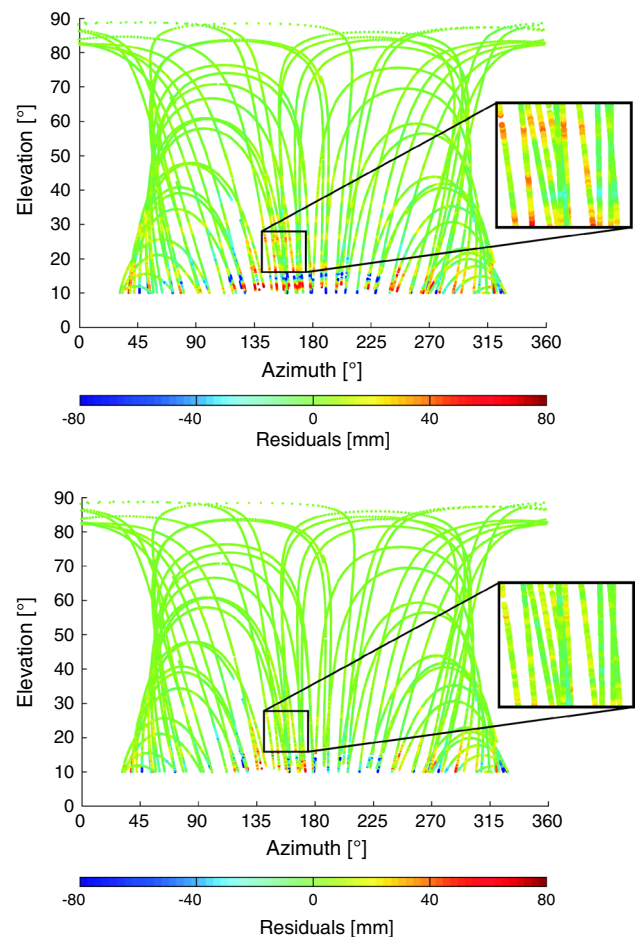

Fig. 5 Residuals before and after multipath correction (site SELESTAT, DOY2008:278). *Top panel* uncorrected residuals, *bottom panel* corrected residuals
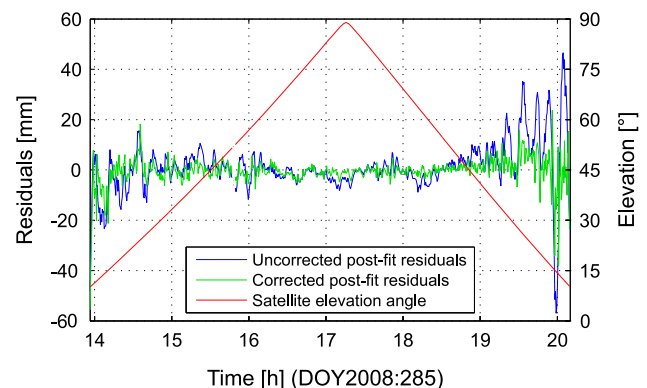

Fig. 6 Time series of residuals before and after multipath correction (site SELESTAT, DOY2008:285, GPS satellite PRN 6)

bottom, the employment of the MPS map significantly reduces the average SD from about 11 mm to 7 mm, corresponding to a relative enhancement of approx. 35 %. Therefore, less variable residuals can be expected if the
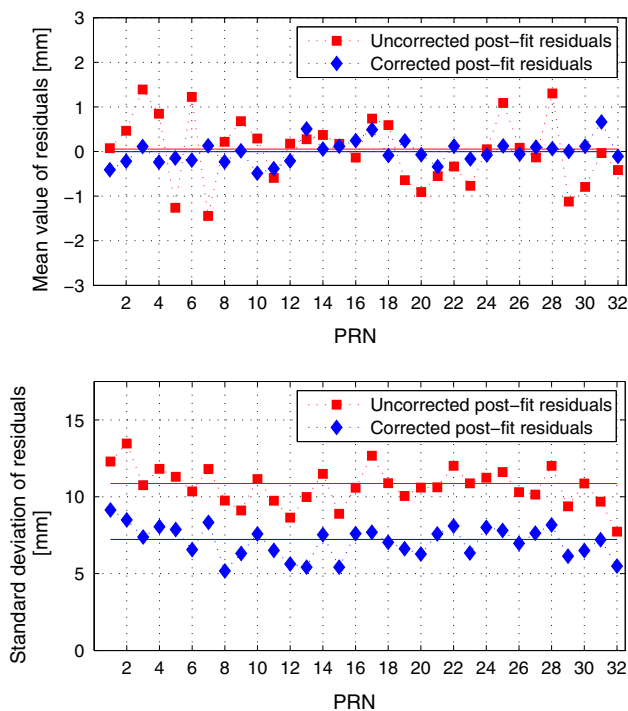
Fig. 7 Satellite-related statistical characteristics of residuals before and after multipath correction (site SELESTAT, DOY2008:276-285) *top panel* arithmetic mean, *bottom panel* SD

Fig. 8 Relative improvement in the SD of residuals before and after multipath correction (DOY2008:276-285) *top panel* all analyzed 61 GURN sites, *bottom panel* site BINGEN with strong multipath effects

multipath correction is performed at the observation level to improve the functional model of GNSS measurements.

Considering different cell resolutions, Fig. 8 compares the relative improvement in the SD of residuals, achieved by means of the conventional and advanced stacking approaches. Taking all 61 GURN sites analyzed into account, Fig. 8, top, illustrates a considerable enhancement of up to about 25 % in the SD of the corrected residuals. This benefit is larger than 35 % for the site BINGEN, see Fig. 8, bottom, a station which is strongly affected by multipath effects even at high elevation angles ($E > 50°$; Knöpfler et al. 2010). Within the framework of the presented case study, the optimal results are achieved using an elevation and azimuth resolution of $0.5° \times 1°$. The advanced stacking approach seems to be superior to the conventional one if the specified cell resolution is better than $1° \times 1°$. In addition, the congruent cell solution is particularly applicable when capturing site-specific effects at high elevations. Although within our approach strict statistical assessments are made before a correction is applied onto the residuals of the cells, the reduction in SDs only differs by about 1 % from a solution without statistical assessment, e.g., subtracting cell mean values even if only two residuals are within the cell. On the other hand, the application of statistical conditions offers the possibility
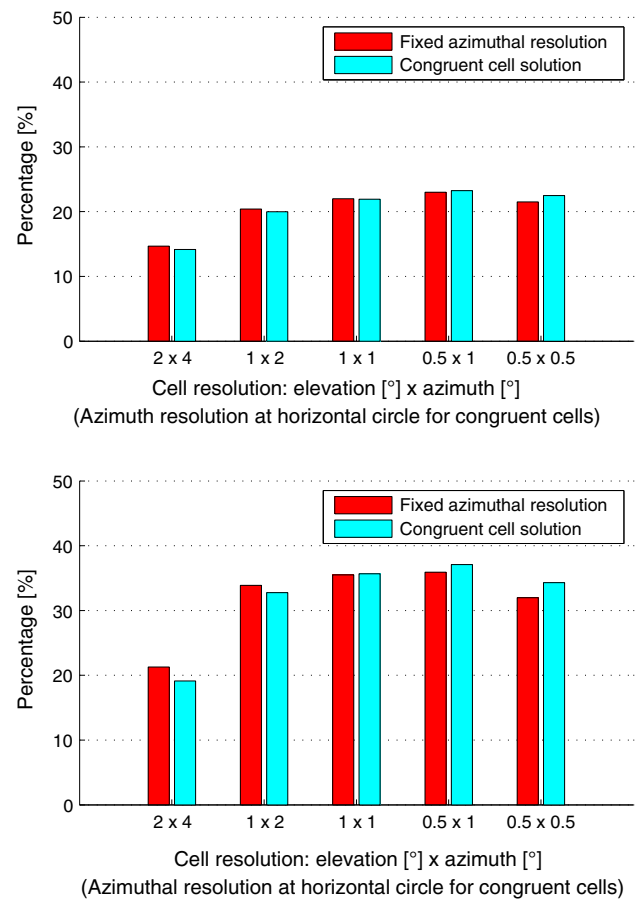
to apply the cell mean values on observations of different days enabling a reliable multipath correction at permanent GNSS sites in real-time.

Conclusions and outlook

We presented a new approach for the generation of residual-based MPS maps focusing on continuously operating GNSS sites. The proposed MPS approach is characterized by two major advantages. First, cell mean values are computed using congruent cells. Second, statistical testing and outlier detection are performed for the calculation of reliable and representative stacked mean values for the cells. As MPS is applied to residuals in the space domain, the approach is easily applicable to all GNSS. In addition, the proposed approach is independent of satellite maneuvers and data tracking rates. The use of congruent cells enables the detection and reduction of far-field multipath effects as well as near-field multipath effects from low- and high-elevation satellites with a high spatial resolution. A

validation of MPS maps at 61 GPS sites proofed a significant reduction of multipath effects in PPP residuals. A comparison with standard MPS approaches, which make use of a fixed azimuthal cell resolution, shows that the MPS approach presented is able to mitigate site-specific errors more appropriate. After the correction of residuals using cell mean values, the SD of residuals was reduced by 38 % at sites with a strong multipath environment. Within our case study, different cell resolutions were applied to PPP residuals of 10 consecutive days at a sample interval of 30 s. The highest reduction of SDs of residuals is achieved using a cell resolution of $0.5° \times 1°$ (elevation $\times$ azimuth at horizontal circle).

The generation of MPS maps is a helpful tool to visualize and interpret multipath signals in the surrounding of a GNSS antenna. In the future, the MPS method developed will be used for the correction of GNSS signals at observation level and for modified observation data evaluation strategies. Because of their statistical robustness, the cell mean values computed from residuals of the past days can be used for real-time correction of observations. As the stacked values comprise all site-specific effects affecting the GNSS antenna, MPS maps also correct for the remaining errors in receiver antenna models. Such corrections of residuals are required, especially if residuals itself are to be exploited, e.g., within the calculation of temporally highly resolved water vapor fields.

References

Agnew DC, Larson KM (2007) Finding the repeat times of the GPS constellation. GPS Solut 11(1):71–76. doi:10.1007/s10291-006-0038-4

Alshawaf F, Fuhrmann T, Heck B, Hinz S, Knöpfler A, Luo X, Mayer M, Schenk A, Thiele A, Westerhaus M (2012) Integration of InSAR and GNSS observations for the determination of atmospheric water vapor. In: Krisp JM et al. (eds), Earth observation of global changes (EOGC), proceedings of EOGC2011, Munich, Germany, 13–15 April, 2011. Lecture Notes in Geoinformation and Cartography, Springer, Berlin, pp 147–162. doi:10.1007/978-3-642-32714-8_10

Bedford L, Brown N, Walford J (2009) New 3D four constellation high performance wideband choke ring antenna. In: Proceedings of ION GNSS 2009, Anaheim, CA, USA, 26–28 Jan 2009, pp 829–835

Bender M, Dick G, Wickert J, Schmidt T, Song S, Gendt G, Ge M, Rothacher M (2008) Validation of GPS slant delays using water vapour radiometers and weather models. Meteorol Z 17(6):807–812. doi:10.1127/0941-2948/2008/0341

Bilich A, Larson KM (2007) Mapping the GPS multipath environment using the signal-to-noise ratio (SNR). Radio Sci 42:RS6003. doi:10.1029/2007RS003652

Braasch MS (1996) Multipath effects. In: Parkinson BW et al. (eds) Global positioning system: theory and applications, vol 1, Am Inst of Aeronaut and Astronaut, Washington DC, Chap. 14

Dach R, Hugentobler U, Fridez P, Meindl M (2007) User manual of the Bernese GPS Software Version 5.0. Astronomical Institute, University of Bern, Stämpfli Publications AG, Bern, Switzerland

Dilßner F, Seeber G, Wübbena G, Schmitz M (2008) Impact of near-field effects on the GNSS position solution. In: Proceedings of ION GNSS 2008, Savannah, GA, USA, 16–19 September 2008, pp 612–624

Eissfeller B, Ameres G, Kropp V, Sanroma D (2007) Performance of GPS, GLONASS and Galileo. In: Fritsch D (ed) Photogrammetric Week 07, Stuttgart, Germany, 3–7 September, 2007, Wichmann, Berlin Offenbach, pp 185–199

Fan KK, Ding XL (2006) Estimation of GPS carrier phase multipath signals based on site environment. J Glob Position Syst 5(1–2): 22–28

Fuhrmann T, Heck B, Knöpfler A, Masson F, Mayer M, Ulrich P, Westerhaus M, Zippelt, K (2012) Recent surface displacements in the Upper Rhine Graben—preliminary results from geodetic networks. Tectonophysics (online first). doi:10.1016/j.tecto.2012.10.012

Fuhrmann T, Knöpfler A, Luo X, Mayer M, Heck B (2010) Zur GNSS-basierten Bestimmung des atmosphärischen Wasserdampfgehalts mittels Precise Point Positioning. Karlsruhe Institute of Technology (KIT) Scientific Reports 7561, KIT Scientific Publishing, Karlsruhe, Germany

Hofmann-Wellenhof B, Lichtenegger H, Wasle E (2008) GNSS-Global Navigation Satellite Systems: GPS, GLONASS, Galileo & more. Springer, Wien

Iwabuchi T, Shoji Y, Shimada S, Nakamura H (2004) Tsukuba GPS Dense Net Campaign observation: improvement in GPS stacking maps of post-fit phase residuals estimated from three software packages. J Meteor Soc Jpn 82(1B):315–330

King MA, Watson CS (2010) Long GPS coordinate time series: multipath and geometry effects. J Geophys Res 115:B04403. doi:10.1029/2009JB006543

Knöpfler A, Masson F, Mayer M, Ulrich P, Heck B (2010) GURN (GNSS Upper Rhine Graben Network)—status and first results. In: Proceedings of FIG Congress 2010, Sydney, Australia, 11–16 April 2010

Lau L (2012) Comparison of measurement and position domain multipath filtering techniques with the repeatable GPS orbits for static antennas. Surv Rev 44(324):9–16. doi:10.1179/1752270611Y.0000000003

Lau L, Cross P (2006) A new signal-to-noise-ratio based stochastic model for GNSS high-precision carrier phase data processing algorithms in the presence of multipath errors. In: Proceedings of ION GNSS 2006, Fort Worth, TX, USA, 26–29 September 2006, pp 276–285

Lidberg M, Eksröm C, Johansson JM (2009) Site-dependent effects in high-accuracy applications of GNSS. EUREF Publication No. 17, Mitteilungen des Bundesamtes für Kartographie und Geodäsie, Band 42, pp 132–138

Liu H, Li X, Ge L, Rizos C, Wang F (2011) Variable length LMS adaptive filter for carrier phase multipath mitigation. GPS Solut 15(1):29–38. doi:10.1007/s10291-010-0165-9

Luo X (2013) GPS stochastic modelling—signal quality measures and ARMA processes. Springer theses: recognizing outstanding Ph.D. research, Springer, Berlin

Luo X, Mayer M, Heck B (2008) Improving the stochastic model of GNSS observations by means of SNR-based weighting. In: Sideris MG (ed) Observing our Changing Earth, Proceedings of the 2007 IAG General Assembly, Perugia, Italy, 2–13 July, 2007, IAG Symposia, vol. 133, Springer, Berlin, pp 725–734. doi:10.1007/978-3-540-85426-5_83

Mayer M, Knöpfler A, Heck B, Masson F, Ulrich P, Ferhat G (2012) GURN (GNSS Upper Rhine Graben Network)—Research Goals and First Results of a Transnational Geo-Scientific Network. In: Kenyon S et al. (eds) Geodesy for planet earth, Proceedings of the 2009 IAG Symposium, Buenos Aires, Argentina, 31 August–September 4, 2009, IAG Symposia, vol. 136, Springer, Berlin, pp 673–681. doi:10.1007/978-3-642-20338-1_83

Niell AE (1996) Global mapping functions for the atmosphere delay at radio wavelengths. J Geophys Res 101(B2):3227–3246. doi:10.1029/95JB03048

Ning T, Elgered G, Johansson JM (2011) The impact of microwave absorber and radome geometries on GNSS measurements of station coordinates and atmospheric water vapour. Adv Space Res 47(2):186–196. doi:10.1016/j.asr.2010.06.023

Park K-D, Elósegui P, Davis JL, Jarlemark POJ, Corey BE, Niell AE, Normandeau JE, Meertens CE, Andreatta VA (2004) Development of an antenna and multipath calibration system for Global Positioning System sites. Radio Sci 39:RS5002. doi:10.1029/2003RS002999

Ragheb AE, Clarke PJ, Edwards SJ (2007) GPS sidereal filtering: coordinate- and carrier-phase-level strategies. J Geod 81(5):325–335. doi:10.1007/s00190-006-0113-1

Ray JK (2006) What receiver technologies exist for mitigating GNSS pseudorange and carrier phase multipath? Inside GNSS 1(6):25–27

Rost C, Wanninger L (2009) Carrier phase multipath mitigation based on GNSS signal quality measurements. J Appl Geod 3(2):81–87. doi:10.1515/JAG.2009.009

Saastamoinen J (1973) Contribution to the theory of atmospheric refraction: Part II. Refraction corrections in satellite geodesy. Bull Geod 107(1):13–34. doi:10.1007/BF02522083

Schmid R, Steigenberger P, Gendt G, Ge M, Rothacher M (2007) Generation of a consistent absolute phase-center correction model for GPS receiver and satellite antennas. J Geod 81(12):781–798. doi:10.1007/s00190-007-0148-y

Seeber G (2003) Satellite geodesy, 2nd edn. Walter de Gruyter, Berlin

Snedecor GW, Cochran WG (1980) Statistical methods, 7th edn. Iowa State University Press, Ames

Wanninger L, May M (2000) Carrier phase multipath calibration of GPS reference stations. In: Proceedings of ION GPS 2000, Salt Lake City, UT, USA, 19–22 September, pp. 132–144

Wübbena G, Schmitz M, Matzke N (2011) On GNSS in situ station calibration of near-field multipath. In: Proceedings of the International Symposium on GNSS, Space-based and Ground-based Augmentation Systems and Applications, Brussels, Belgium, 29–30 November, 2010

Zhong P, Ding XL, Zheng DW, Chen W, Huang DF (2008) Adaptive wavelet transform based on cross-validation method and its application to GPS multipath mitigation. GPS Solut 12(2):109–117. doi:10.1007/s10291-007-0071-y

Zumberge JF, Heflin MB, Jefferson DC, Watkins MM, Webb FH (1997) Precise point positioning for the efficient and robust analysis of GPS data from large networks. J Geophys Res 102(B3):5005–5017. doi:10.1029/96JB03860

Thomas Fuhrmann received his Diploma in Geodesy and Geoinformatics in 2010 studying GNSS-based estimation of water vapor using precise point positioning. He is currently working on a project to detect crustal deformations from analysis of leveling, InSAR, and GNSS data at the Geodetic Institute of the Karlsruhe Institute of Technology (KIT), Germany.

Xiaoguang Luo received the PhD degree in geodesy from Karlsruhe Institute of Technology (KIT), Germany, in 2012. Since September 2013, he has been a GNSS Application Engineer of the GNSS Product Management Group, Leica Geosystems. His research interests include analysis of stochastic models, and atmospheric and site-specific effects of GNSS observations, with a special focus on statistical testing and time-series modeling.

Andreas Knöpfler is a member of the Geodetic Institute of the Karlsruhe Institute of Technology (KIT), Germany, and received his Diploma in Geodesy and Geoinformatics in 2005. He is working on GNSS in science and education with a special focus on geodynamics and site-specific effects.

Michael Mayer received his doctoral degree in 2005 from the Karlsruhe University (TH), where he was researching the modeling of the GPS deformation network Antarctic Peninsula. He is head of the GNSS working group of the Geodetic Institute and interested in mitigation of atmospheric and site-specific GNSS effects with a special focus on continuously operated reference sites.